Full Research Paper

Simulation of Optical Microfiber Loop Resonators for Ambient Refractive Index Sensing

Lei Shi, Yonghao Xu, Wei Tan and Xianfeng Chen*

Department of Physics, the State Key Laboratory on Fiber Optic Local Area Communication Networks and Advanced Optical Communication Systems, Shanghai Jiao Tong University, Shanghai 200240, China

* Author to whom correspondence should be addressed; E-mail: xfchen@sjtu.edu.cn

Abstract: Based on theoretical modeling and optimization, we exploit the application of optical microfiber loop resonators in ambient refractive index sensing. We set up a reliable theoretical model and optimize the structural parameters of microfiber loop resonators including the radius of the microrfiber, the radius of the loop and the length of the coupling region for higher sensitivity, wider dynamic measurement range, and lower detection limit. To show the convincible and realizable sensing ability we perform the simulation of sensing an extreme small variation of ambient refractive index by employing a set of experimental data as the parameters in the expression of intensity transmission coefficient, and the detection limit reaches to a variation of ambient refractive index of 10^{-5} refractive index unit (RIU). This has superiority over the existing evanescent field-based subwavelength-diameter optical fiber refractive index sensor.

Keywords: Fiber optics sensors; Optical resonators; Subwavelength-diameter optical fibers.

1. Introduction

Recently optical waveguides with subwavelength diameter attract much attention, especially optical microfiber-based photonic devices [1-6]. Fabrication methods of ultra-high-quality silica optical microfibers with length up to ~10cm and diameter down to ~30nm have been developed [2-3, 6], so silica optical microfibers are promising to develop micro- and nano-photonic devices. Demonstrated and potential applications of microfibers include nonlinear optics[3,7-8], optical sensing[9-11], and the

microfiber loop resonator(MLR)[12-17].Compared to integrated optical waveguide ring resonators[18], MLRs are more convenient for fabrication, manipulation and application. An MLR can be directly obtained using a microfiber manipulated into a loop, where effective coupling occurs between the contact sections of the microfiber. The MLR with loaded *Q*-factor of 120000 has been produced [16], and the performance is close to that of integrated waveguide micro-ring resonators of which the largest *Q*-factor has been demonstrated recently [19].

MLRs are also potentially useful for optical filtering, active devices and optical sensing as the integrated waveguide micro-ring resonators [18]. However, the research on MLRs for ambient refractive index sensing hasn't been reported. In this paper, we simulate the response of MLRs to the variation of ambient refractive index and optimize the structural parameters of MLRs to provide a theoretical guide for variant requirements in practical sensing applications. After that we perform the simulation based on a set of experimental data in reference [16] to show the achievable sensing performance of MLRs.
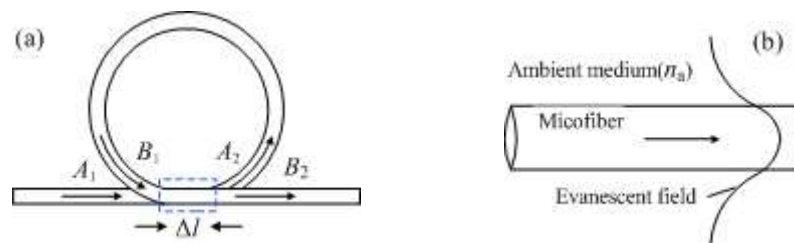
Figure 1. (a) Geometry of of an MLR and (b) Optical signal transmits in a microfiber with the ambient refractive index n_a.

2. Theory

2.1. Fundamental s of an MLR

A typical MLR is shown in Fig. 1(a). A_1, A_2, B_1 and B_2 are the complex mode amplitudes. Coupling of optical signal occurs in the region selected by the blue dashed line frame, where the adjacent microfibers contact are parallel with each other. The loop can be treated as a circle, and then the length of the loop L is equal to $2\pi R$, where R is the radius of the loop.

For simplicity the polarization effect is ignored [16]. Based on the fact that fabrication of ultra-low-loss silica microfibers with length up to ~10cm and uniform diameter has been demonstrated [2-3,6], we can assume that the field distribution in the loop is independent on the specific axial position for the theoretical simulation. That is to say, both propagation constant β and coupling coefficient κ are constant functions of the axial position.

The intensity transmission coefficient T, representing the ratio of the transmission intensity to the input intensity, can be obtained according to general principle of ring resonators [16, 22-23] and has the expression [16]

$$T = \left|\frac{B_2}{A_1}\right|^2 = \left|\frac{\exp(-\frac{\alpha L}{2})\exp(i\varphi) - \sin(K)}{1 - \sin(K)\exp(-\frac{\alpha L}{2})\exp(i\varphi)}\right|^2$$

$$= \frac{\exp(-\alpha L) + (\sin(K))^2 - 2\exp(-\alpha L/2)\sin(K)\cos(\varphi)}{1 + \exp(-\alpha L)(\sin(K))^2 - 2\exp(-\alpha L/2)\sin(K)\cos(\varphi)}$$

(1)

where α is the intensity attenuation coefficient (*viz.* power attenuation coefficient for this model), L is the length of the loop, φ is the roundtrip phase shift, K is the coupling parameter. For the field distribution in the microfiber is independent on the axial position we can get $\varphi=\beta L$ and $K=\kappa\Delta l$, where Δl is the length of the coupling region.

From the expression of T, we know the resonances in transmission spectrum generate when $\cos(\varphi)$ is equal to zero and the coupling parameter K is close to $K_m=(2m+1)\pi/2$, where m is an integer [16,22-23].

The free spectrum range(FSR) of an MLR, which is defined as the spacing between adjacent resonant wavelengths, and the *Q*-factor of an MLR, which is defined as of resonant wavelength λ to the full width at half maximum of the corresponding resonance spectrum, can be respectively expressed as when $\alpha L \ll 1$ [16]

$$Q = \frac{\lambda L}{(K - K_m)^2 + \alpha L} \cdot \frac{\partial \beta}{\partial \lambda}, \quad FSR = \frac{2\pi}{L} \cdot \frac{1}{\frac{\partial \beta}{\partial \lambda}}$$

(2)

2.2. Sensing Parameters

The sensing mechanism of MLR-based biochemical sensors is based on the shift of resonant wavelength λ_r due to a variation of ambient refractive index caused by varied ambient material concentration, and it is illustrated in Fig. 1(b). The microfiber is so thin that fractional optical power transmits in the ambient cladding [9]. As the refractive index of ambient material n_a changes the effective index of the guided modes in the microfiber n_{eff} is modified, and then the resonant wavelength shifts.

Following the sensing mechanism the sensitivity can be defined as [20]

$$S = \frac{\partial \lambda_r}{\partial n_a} = \frac{\partial \lambda_r}{\partial n_{eff}} \cdot \frac{\partial n_{eff}}{\partial n_a}$$

(3)

Another important parameter for sensing applications is the detection limit δn_a. According to the definition of sensitivity the detection limit has the feature [20]

$$\delta n_a \sim \delta \lambda_r \cdot \frac{\partial n_a}{\partial \lambda_r} \rightarrow \delta n_a \propto \frac{1}{S}$$

(4)

where $\delta\lambda_r$ is the spectral resolution of the measurement system. Theoretically the higher S is, the smaller the detection limit is. However, in fact it is very difficult to exactly obtain the shift of the resonant wavelength if the spectrum width is large, for the experimental line shape usually does not agree with the theoretical line shape so well. So only if the Q-factor is high enough the low detection limit can be achievable, and we define the detection limit factor $P = Q \cdot S$ [20] to characterize the detection limit. The larger P is, the lower the detection limit is.

3. Optimization of the Structural Parameters of the MLR for Ambient Refractive Index Sensing

From (2), (3) and (4) we know that the sensing parameters sensitivity and detection limit are determined by several key structural parameters of the MLR: the radius of the microfiber a, the radius of the loop R and the length of the coupling region Δl, so we perform our simulations to optimize these parameters for high-performance sensing.

The operation wavelength is set in ~1.55μm, and we choose the radius of microfibers ranging from 0.3μm to 0.55μm to satisfy single mode operation and low loss for our simulations.

For the intrinsic loss of microfibers is ultra low we only consider the attenuation due to bend loss for α [21], and κ can be obtained from the coupled-mode theory [16, 21].

At first we pay attention to the sensitivity. From (3) the sensitivity is related to the radius of the microfiber and the loop. The results shown in Fig. 2(a) indicate that the sensitivity increases as the radius of the microfiber decreases, and hardly changes with the radius of the loop. Microfibers with smaller radius have higher fractional power transmitting in the ambient cladding, and then are more sensitive to the variation of ambient refractive index. As to the radius of the loop, $\partial n_{eff}/\partial n_a$ in (3) is independent on R, and $\partial \lambda_r/\partial n_{eff}$ in (3) is hardly dependent on R, which can be understood from the first resonance condition. Moreover, from (4) the theoretical detection limit is a variation of ~10^{-6} RIU based on an optical spectrum analyzer with the resolution of 1pm as the measurement apparatus.

For sensing applications, wide dynamic measurement range is also important, and it is related to the FSR based on this sensing mechanism. From the definition FSR is independent on the coupling parameter, and its evolution trend is shown in Fig. 2(b). Small a and R are necessary to obtain larger FSR, and R is the dominant factor, which can be understood from the definition of FSR.
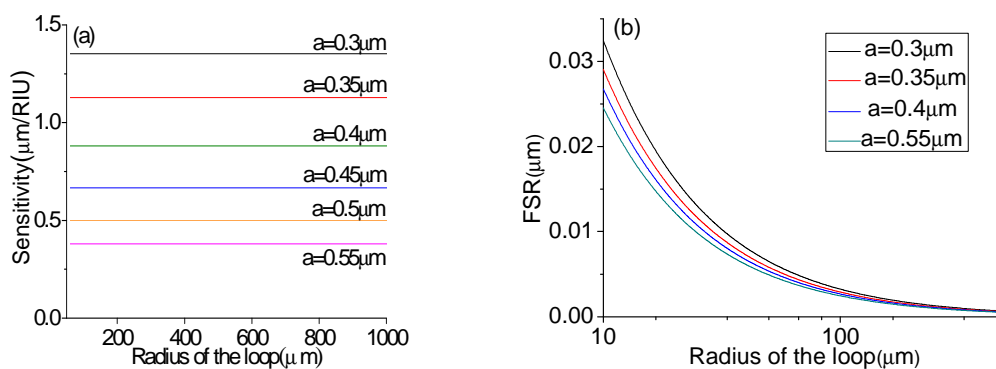
Figure 2. (a) Sensitivity versus the radius of the loop R and the radius of the microfiber a, the unit of sensitivity is μm per refractive index unit (RIU) (b) FSR versus the radius of the loop R and the radius of the microfiber a.

Q-factor is the most important parameter for a resonator for it characterizes the performance of a resonator. Though the asymptotic formula of power attenuation coefficient α is not accurate enough when the radius of the loop is very small (e.g. $a{\sim}10\mu m$) [4], it is still reliable to simulate the evolution trend of the Q-factor and the detection limit factor P as the structural parameters of the MLR change.

From (3) we know Q-factor depends on a, R and Δl. The results shown in Fig. 3(a) indicate that higher Q-factor corresponds to large R and large a. In fact the Q-factor linearly depends on R if we use conventional linear scale instead of logarithm scale, and this is similar to integrated waveguide micro-ring resonators [24]. High Q-factor also can be obtained based on large a for corresponding lower loss when R is large. The coupling length Δl is another important parameter that affects the Q-factor. The coupling parameter K is periodic function of Δl, and $(K\text{-}K_m)^2$ is the same. So Q-factor is modified periodically as the coupling length changes. We come to a conclusion that the coupling length Δl which makes K close to K_m is necessary to obtain higher Q-factor.
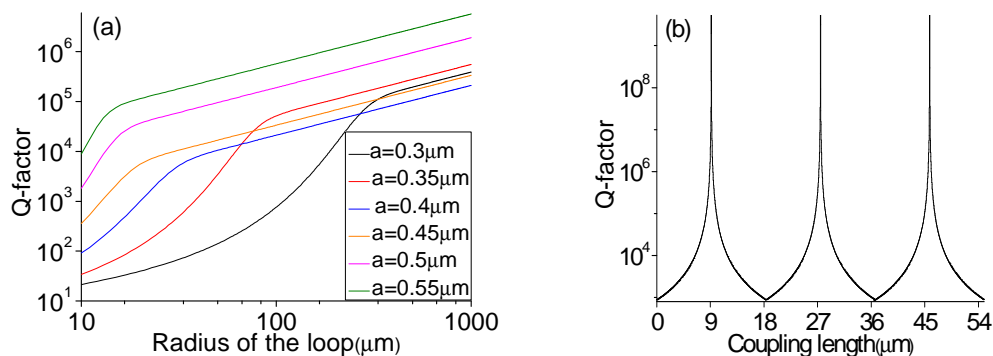
Figure 3. (a) Q-factor versus the radius of the loop R and the radius of the microfiber a, fixed parameter Δl=10μm (b) Q-factor versus the coupling length Δl, fixed parameters a=0.5μm, R=55μm.
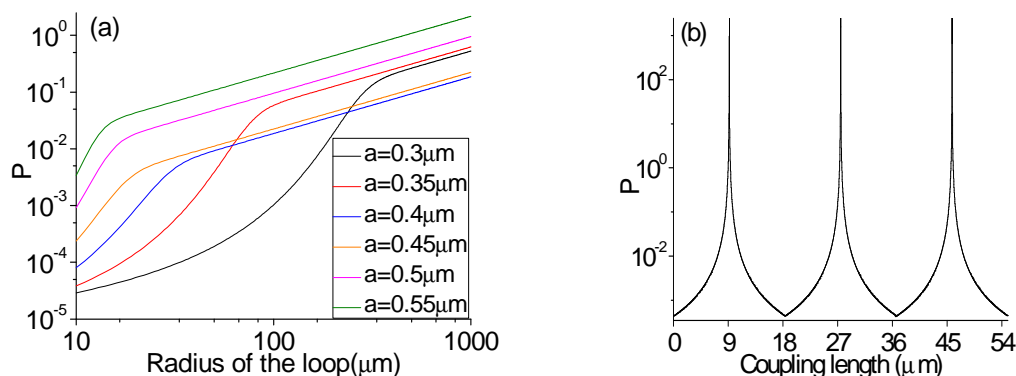
Figure 4. (a) The detection limit factor P versus the radius of the loop R, fixed parameter Δl=10μm. (b) The detection limit P versus the coupling length Δl, fixed parameters a=0.5μm, R=55μm.

At last the detection limit factor is calculated. It is shown in Fig. 4 that the evolution trend of detection limit factor is similar to that of Q-factor. Lower detection limit can be obtained by choosing large a, large R and appropriate Δl. According to the preceding discussion the detection limit is in the

inverse ratio of both *Q*-factor and the sensitivity. However, these two parameters have inverse dependences on the radius of the microfiber, so we should to find a balance between them. The results indicate that the detection limit factor has similar trend to that of the *Q*-factor. That is to say, the *Q*-factor is the dominant parameter for affecting the detection limit.

Based on the foregoing simulations we find the structural parameters of MLRs which correspond to better sensing performance following our variant practical requirements.

4. Simulation of Sensing an Extreme Small Variation of Ambient Refractive Index

To show the convincible and realizable sensing ability we perform the simulation employing a set of experimental data in reference [16] as the parameters in equation (1). The radius of the microfiber is 0.45μm and the length of the loop is 2mm. Corresponding roundtrip attenuation *αL* is 0.14 and amplitude coupling coefficient sin(*K*) is 0.981 with operation wavelength ~1.55μm [16]. The resolution of an optical spectrum analyzer is 1pm, so we can obtain that the detection limit of this MLR-based sensor is an ambient refractive index variation of 10^{-5} RIU from the simulation results shown in Fig. 5. It is indicated that the MLR-based sensor has superiority over the existing evanescent field-based subwavelength-diameter optical fiber refractive index sensor of which the detection limit is a variation of ~10^{4}RIU[11]. As the improvement of fabrication technology of MLRs, we believe the theoretical detection limit of ~10^{-6}RIU is achievable.
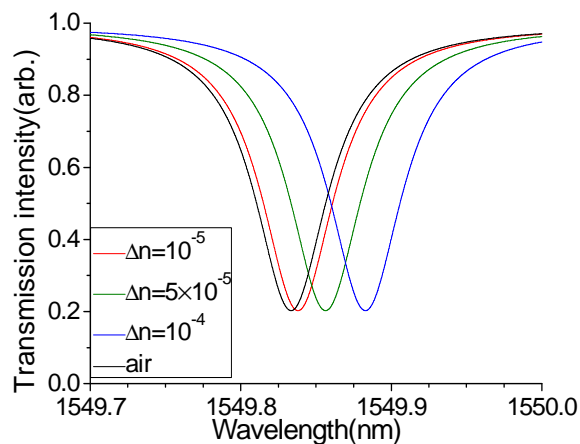
Figure 5. Sensing an extreme small variation of ambient refractive index.

5. Conclusion

We simulate the dependence of sensing performance on the structural parameters of MLRs and conclude that higher *Q*-factor corresponds to large *a*, large *R* and appropriate Δ*l*, higher sensitivity which is hardly dependent on *R* corresponds to small *a*, and lower detection limit corresponds to large *a*, large *R* and appropriate Δ*l*. After that we perform the simulation of sensing ambient refractive index according to a set of experimental data in reference [16] to show the reachable sensing ability of the MLR-based sensor, and the results indicate the detection limit reaches to a variation of 10^{-5} RIU. It precedes the demonstrated submicron-diameter optical fiber refractive index sensor. It is indicated that

the microfiber loop resonator-based ambient refractive index sensor is a kind of promising photonic device.

Acknowledgements

References

1. Tong, L.; Ashcom, J.B.; He, S.L.; Lou, J.Y.; Shen, M.Y.; Maxwell, I.; Mazur, E. Subwavelength-diameter silica wires for low-loss optical waveguiding. *Nature* **2003**, *426*, 816-819.
2. Brambilla, G.; Finazz, V.; Richardson, D. J. Ultra-low-loss optical fiber nanotapers. *Opt. Express* **2004**, *12*, 2258-2263.
3. Leon-Saval, S.G.; Birks, T. A.; Wadsworth, W. J.; Russell, P. St. J. Supercontinuum generation in submicron fibre waveguides. *Opt. Express* **2004**, *12*, 2864-2869.
4. Sumetsky, M.; Dulashko, Y.; Hale, A. Fabrication and study of bent and coiled free silica nanowires: Self-coupling microloop optical interferometer. *Opt. Express* **2004**, *12*, 3521-3531.
5. Law, M.; Sirbuly, D.J.; Johnson, J.C.; Goldberger, J.; Saykally, R.J.; Yang, P.D. Nanoribbon waveguides for subwavelength photonics integration. *Science* **2004**, *305*,1269-1273.
6. Brambilla, G.; Xu, F.; Feng, X. Fabrication of optical fiber nanowires and their optical and mechanical Characterization. *Electron. Lett.* **2006**, *42*, 517-51.
7. Foster, M.A.; Gaeta, A. L. Soliton-effect compress of supercontinuum to few-cycle durations in photonic nanowires. *Opt. Express* **2005**, *13*, 6848-6855.
8. Gattass, R.R.; Svacha, G. T.; Tong, L.; Mazur, E. Supercontinuum generation in submicrometer diameter silica fibers. *Opt. Express* **2006**, *14*, 9048-9014.
9. Lou, J.; Tong, L.; Ye, Z. Modeling of silica nanowires for optical sensing. *Opt. Express* **2005,** *13*,213-2140.
10. Villatoro, J.; Monzon-hernandez, D. Fast detection of hydrogen with nano fiber tapers coated with ultra thin palladium layers. *Opt. Express* **2004**, *13*, 5087-5092.
11. Polynkin, P.; Polykin, A.; Peyghambarian, N.; Mansuripur, M. Evanescent field-based optical fiber sensing devices for measuring the refractive index of liquid in microfluidic channels. *Opt. Lett.* **2005**, *30*, 1273-1275.
12. Sumetsky, M. Optical fiber microcoil resonator.*Opt. Experss* **2004**, *12*, 2303-2316.
13. Sumetsky, M.; Dulashko, Y.; Fini ,J.M.; Hale, A. Optical microfiber loop resonator. *Appl. Phys. Lett.* **2005**, *86*, 161108.
14. Sumetsky, M. Uniform coil optical resonator and waveguide: Transmission spectrum,eigenmodes, and dispersion relation. *Opt. Express* **2005**, *13*, 4331-4340.
15. Sumetsky, M.; Dulashko, Y.; Fini, J. M.; Hale, A.; DiGiovanni, D. J. Demonstration of a microfiber loop resonator. *Optical Fiber Communications Conference* (*Optical Society of America*, *Anaheim*, *CA*, **2005**), Postdeadline Paper PDP10.
16. Sumetsky, M.; Dulashko, Y.; Hale, A.; DiGiovanni, D.J. The microfiber loop resonator: theory, experiment, and application. *J. Lightw. Technol.* **2006**, *24*, 242-250.

17. Jiang, X.; Tong, L.; Vienne, G.; Guo, X. Demonstration of optical knot resontors. *Appl. Phys. Lett.* **2006**, *88*, 223501.

18. Vahala, K. J. Optical microcavities. *Nature* **2003**, *424*, 839-846.

19. Niehusmann, J.; Vorckel, A.; Bolivar, P.H.; Wahlbrink, T.; Henschel, W. and Kurz, H. Ultrahighquality-factor silicon-on-insulator microring resonator. *Opt. Lett.* **2004**, *29*, 2861-2863.

20. Chao, C. Y.; Guo, L. J. Design and optimization of microring resonators in biochemical sensing applications. *J. Lightw. Technol.* **2006**, *24*, 1395-1402.

21. Snyder, A.W.; Love, J.D. *Optical Waveguide Theory*; Chapman & Hall: London, 1983.

22. Stokes, L. F.; Chodorow, M.; Shaw, H. J. All-single-mode fiber resonator. *Opt. Lett.* **1982**, *7*, 288-290.

23. Schwelb, O. Transmission, group delay, and dispersion in single-ring optical resonators and add/drop filters - A tutorial overview. *J. Lightw. Technol.* **2004**, *22*, 1380-1394.

24. Little, B. E.; Chu, S. T.; Haus, H. A.; Foresi, J.; Laine, J. P. Microring resonator channel dropping filters. *J. Lightw. Technol.* **1997**, *15*, 998-1005.